AAS 01-303

CONTINUATION OF PERIODIC ORBITS AROUND LAGRANGE POINTS AND AUTO2000

R. C. Paffenroth,[*] E. J. Doedel,[†] D. J. Dichmann[‡]

September 19, 2001

Abstract

AUTO is a software tool for continuation and bifurcation problems in ordinary differential equations, originally written in 1980 and widely used in the dynamical systems community. In this paper we discuss the parameter continuation algorithms that underlie the AUTO2000 software and demonstrate how they may be applied to the gravitational Circular Restricted 3-Body Problem (CR3BP). Our computational focus is families of periodic orbits which emanate from the L1 Lagrange point in the CR3BP.

INTRODUCTION

In dynamical systems we can gain a basic understanding of the dynamics by identifying elementary solutions such as equilibria and periodic solutions, and determining how such solutions vary with the system parameters. In this paper we show how boundary value continuation software such as AUTO,[8] and more recently AUTO2000,[11] can be used to compute families of periodic solutions of conservative systems, i.e., systems having a first integral. The method is applicable to the computation of periodic solutions of the Circular Restricted 3-Body Problem (CR3BP). The basic idea of the method is very simple and hardly new. It can be found, albeit without detailed mention, in Doedel.[6] Subsequently the continuation method described in this paper has been used in many other applications; as two examples we mention Zufiría[36] and Doedel et al.[7] In addition, a more extensive analysis of the ideas in this paper can be found in Doedel et al.[12]

The computation at the heart of many mathematical models of physical systems is the solution of a parameter-dependent system of nonlinear equations. Such problems generally have more than one solution, and it is often desirable to compute a set of solutions and search for specific solutions with certainly desirable properties. We call the solution set for such a problem a bifurcation diagram. The computation of such bifurcation diagrams and their singularities, e.g., folds, bifurcation points etc., is the domain of numerical parameter continuation algorithms. AUTO2000 is a program which computes such bifurcation diagrams, and has applications ranging from fluid dynamics, cardiac electrophysiology, continuum models of large bio-molecules, and the gravitational N-body problem, to name but a few.

[*] Applied and Computational Mathematics, California Institute of Technology
[†] Department of Computer Science, Concordia University
[‡] Consultant, Torrance CA

Our main example involves the computation of periodic orbits as Hopf bifurcations from the Lagrange points in the CR3BP problem.[16,17] This problem is Hamiltonian, so the continuation methods implemented in AUTO2000 are not immediately applicable. One cannot apply such methods because the existence of first integrals implies non-uniqueness of solutions when the problem is phrased as a two-point boundary value problem in the obvious way. In this paper we describe how such boundary value problems may be modified to account for the Hamiltonian structure. We give a very simple example to illustrate the principal idea used in the computation of families of periodic solutions of conservative systems. We also show how the CR3BP problem may be reformulated using the above ideas so that we may apply numerical continuation methods.

Families of periodic orbits can be computed by continuation methods over a wide range of energy values. Numerical continuation methods are not restricted to a neighborhood of the Lagrange point, do not depend on any symmetry properties of the solution, and can compute periodic orbits of arbitrary extent until some singularity is reached, such as a collision with a primary. AUTO2000 provides for detection and continuation of bifurcating branches of solutions, so a detailed map of periodic orbits may be computed for each of the Lagrange points for any given value of the ratio of the masses of the primaries. As the main result of this paper, we graphically illustrate the solution structure of periodic orbits of the CR3BP in three space dimensions. These periodic orbits include the Lyapunov orbits of the two-space-dimension model. However, the three-space dimension model has a much richer periodic solution structure, containing many bifurcations that can be detected easily in our two-point boundary value problem continuation approach. The resulting bifurcation diagram contains some well-known solutions such as the halo orbits, whose behavior and stability properties have been computed before. (See, for example Howell[21] for a detailed numerical study.)

The AUTO2000 source code is publicly available via HTTP from the web site:

http://auto2000.sourceforge.net.

CONTINUATION OF SOLUTIONS

Most existing numerical continuation algorithms are for the computation of one-dimensional solution manifolds called *solution branches*, e.g., Allgower and Georg,[1] Doedel et al.[9,10] and Rheinboldt.[30] However, continuation algorithms have also been developed for higher-dimensional manifolds; see, in particular, the recent paper by Henderson,[19] and references therein. In our paper we only consider the computation of solution branches.

To recall the basic notions of continuation, first consider the finite-dimensional equation

$$F(X) = 0, \qquad F \; : \; \mathbb{R}^{n+1} \; \to \; \mathbb{R}^n, \tag{1}$$

where F is assumed to be sufficiently smooth for the theory to apply. This system has one more variable than it has equations. Given a solution X_0, there generally exists a locally unique one-dimensional family of points, called a solution branch, that passes through X_0. To compute another nearby point X_1 on this branch, one can designate one component of X_0 as the *continuation parameter* λ and write

$$X_0 = (Y_0, \lambda_0), \quad \text{where} \quad Y_0 \in \mathbb{R}^n, \quad \text{and} \quad \lambda_0 \in \mathbb{R}. \tag{2}$$

One can then use some root finding procedure, such as Newton's method, to solve the extended system

$$\begin{array}{ll} \text{a)} & F(X_1) = 0, \\ \text{b)} & \lambda_1 - \lambda_0 = \Delta\lambda \end{array} \tag{3}$$

using as an initial guess $X_1^{\#} = (Y_0, \lambda_1)$. In general $F(X_1^{\#}) \neq 0$, but if the step size $\Delta\lambda$ is sufficiently small, and F is sufficiently smooth, then $X_1^{\#}$ lies within the basin of attraction of the given root finding procedure, so the procedure converges to X_1. This algorithm is called *natural parameter continuation* and is shown schematically in Figure 1.

Natural parameter continuation captures the central ideas of numerical continuation, but it has some weaknesses. One significant problem with natural parameter continuation is that it fails at a *fold*, i.e. a place where the solution curve is not a function of the parameter λ, as shown in Figure 2. Natural continuation can fail because it does not account for the local shape of the solution curve.

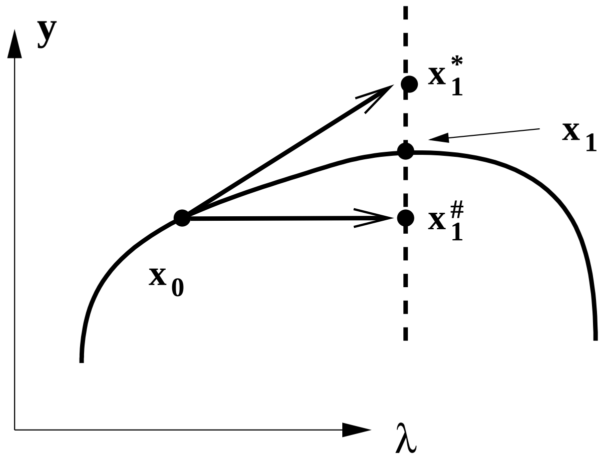

Figure 1: Natural continuation with two different guesses: Solving Equation 3 using Newton's method entails the selection of an initial approximation. For example, one can use the approximation $X_1^{\#} = (Y_0, \lambda_1)$. On the other hand, one might want to use a higher order approximation. For example, given $\dot{X}_0$, the unit tangent to the solution curve at X_0, one can use $X_1 = X_0 + \dot{X}_0\ \alpha$ as a more accurate initial approximation, where α is chosen to have X_1 lie on the line $\lambda = \lambda_1$.

To formulate a method which can compute folds, we begin by constructing a better initial approximation to X_1 as $X_1^* = X_0 + \dot{X}_0 \Delta s$ for some stepsize Δs. Here $\dot{X}_0$ is the unit tangent to the solution curve at X_0. If we differentiate Equation (1) with respect to the arclength s at X_0, we find $F_X(X_0)\ \dot{X}_0 = 0$. Thus the vector $\dot{X}_0$ is a null vector of the Jacobian matrix $F_X(X_0)$, and can be computed at little cost. However as shown in Figure 2, the higher order approximation does not, by itself, suffice because there may be no solutions for the fixed value of λ. One must allow values of λ to be determined by the geometry of the solution curve. Accordingly, we replace the system in Equation 3 with

$$\begin{aligned} &\text{a)}\quad F(X_1) = 0, \\ &\text{b)}\quad (X_1 - X_0)^T \dot{X}_0 = \Delta s, \end{aligned} \tag{4}$$

where the superscript T denotes the transpose. The size of the step size Δs is normally adapted along the branch, depending on the convergence rate of Newton's method. The result is a well-known algorithm, called the *pseudo-arclength continuation method*,[27] and is shown schematically in Figure 3. The name pseudo-arclength arises from the fact that the stepsize Δs approximates the arclength along the curve.

It can be shown that the above continuation method works if X_0 is a *regular solution*, i.e., if the null space of $F_X(X_0)$ is one-dimensional. In this case the Jacobian of Equation 4 evaluated at X_0,

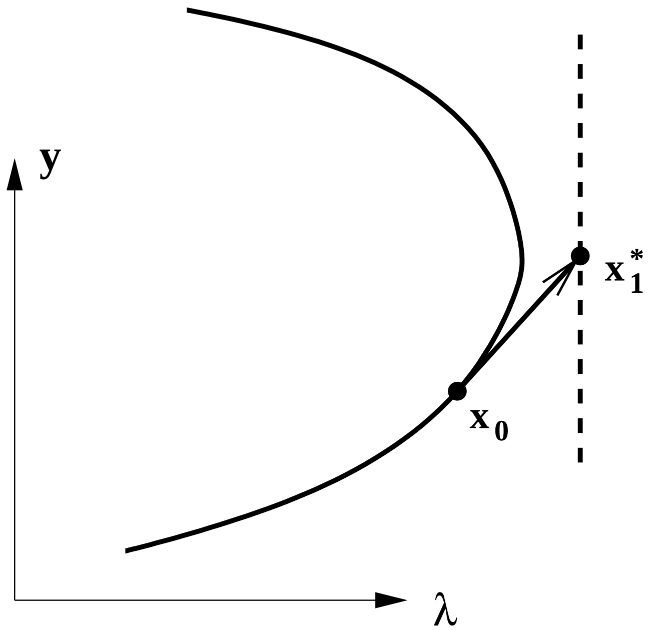

Figure 2: Natural parameter continuation and folds: A fold with respect to λ is a point at which the solution branch is not locally parameterizable by λ. As a consequence, the natural continuation method, which attempts to compute a solution for a fixed value of λ, may fail.

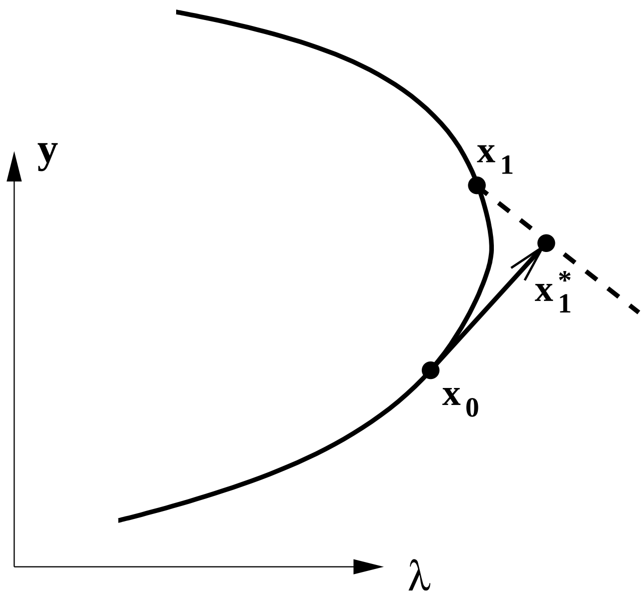

Figure 3: Pseudo-arclength continuation: Instead of fixing the value of λ, we add a constraint as shown in Equation 4b which implies the new solution X_1 we compute lies in the hyperplane perpendicular to the tangent vector $\dot{X}_0$. In this way, the value of λ is allowed to vary, and is computed as one of the solution components using Newton's method.

i.e., the $n+1$ by $n+1$ matrix

$$\begin{pmatrix} F_X(X_0) \\ \dot{X}_0^T \end{pmatrix}, \tag{5}$$

can be easily shown to be nonsingular. By the Implicit Function Theorem, this guarantees the existence of a locally unique solution branch through X_0. This branch can be parameterized locally by Δs. Moreover, for Δs sufficiently small and the initial approximation $X_1^{(0)} = X_0 + \dot{X}_0 \Delta s$, Newton's method for solving (4) can be shown to converge.

One may now iterate this procedure: X_0 is used to compute X_1, which in turn in used to compute X_2, etc. As shown in Figure 4, the core principle of numerical continuation is that for a sufficiently smooth F the solution branch is surrounded by a basin of attraction for Newton's method. If we have some starting value X_0 on the solution branch, then all steps stay within the basin of attraction and Newton's method converges for all steps of the calculation. On the other hand, if one were to directly search for a solution where $\lambda = \lambda_{desired}$, and one did not have a good initial approximation, then there is no guarantee Newton's method would converge.

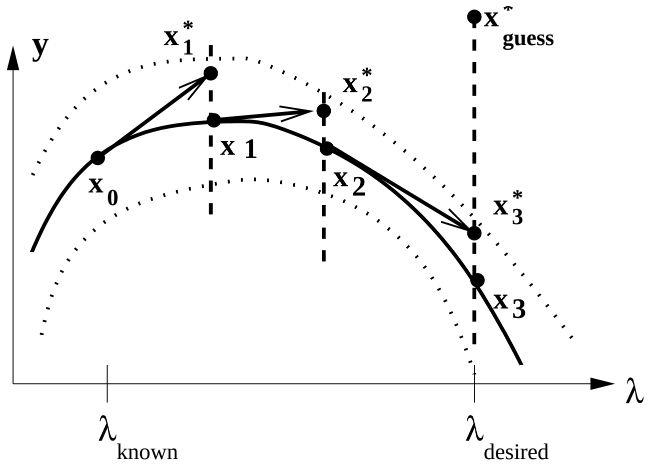

Figure 4: Staying within the basin of attraction: The core principle of numerical continuation is that for a sufficiently smooth F a solution branch comprised of regular solutions is surrounded by a basin of attraction for Newton's method, shown here as the region bounded by dotted lines. If we have have some starting value X_0 on the solution branch, then stepsizes can be chosen so that all steps stay within the basin of attraction and Newton's method converges. On the other hand, if one were to directly search for a solution where $\lambda = \lambda_{desired}$, and did not have a good initial approximation such as X^*_{guess}, then there is no guarantee Newton's method would converge.

In this paper we focus on the problem of computing a branch of periodic solutions of a dynamical system

$$x'(t) = f\big(x(t), \lambda\big), \qquad f \,:\, \mathbb{R}^n \times \mathbb{R} \,\to\, \mathbb{R}^n, \tag{6}$$

where $\lambda \in \mathbb{R}$ is a physical parameter. In this case the continuation step corresponding to Equation 4 takes the form of the constrained periodic boundary value problem

$$\begin{array}{ll} \mathrm{a}_1) & x_1'(\tau) = T_1 f\big(x_1(\tau), \lambda_1\big), \\ \mathrm{a}_2) & x_1(0) = x_1(1), \\ \mathrm{a}_3) & \int_0^1 x_1(\tau)^T \, x_0'(\tau) \; d\tau = 0, \\ \mathrm{b}) & \int_0^1 \big(x_1(\tau) - x_0(\tau)\big)^T \dot{x}_0(\tau) \; d\tau + (T_1 - T_0)\dot{T}_0 + (\lambda_1 - \lambda_0)\dot{\lambda}_0 = \Delta s, \end{array} \tag{7}$$

for $X_1 = (x_1(\cdot), T_1, \lambda_1)$, given a solution $X_0 = (x_0(\cdot), T_0, \lambda_0)$ and its tangent to the solution branch $\dot{X}_0 = (\dot{x}_0(\cdot), \dot{T}_0, \dot{\lambda}_0)$. Here $T_1 \in \mathbb{R}$ is the unknown period, and $\tau \in \mathbb{R}$ is a scaled independent variable such that the periodic solution has period one as a function of τ. Equation 7a$_2$ imposes unit periodicity. Equation 7a$_3$ is a phase condition, which fixes the phase of the new orbit $x_1(\cdot)$ relative to the given orbit $x_0(\cdot)$. This integral phase condition has the desirable property of minimizing phase drift relative to $x_0(\cdot)$. Equation 7b is the functional form of the pseudo-arclength constraint 4b. For full details on this formulation see Doedel et al.[10]

For each continuation step, Equation 7 can be solved by numerical boundary value solvers. In particular, AUTO[8] uses piecewise polynomial collocation, similar to COLSYS,[2] with adaptive mesh selection; see Russell and Christiansen.[33]

PERIODIC SOLUTIONS OF CONSERVATIVE SYSTEMS

The Circular Restricted 3-Body Problem (CR3BP) is an example of a conservative system, where there exists a nondegenerate first integral. Such systems have special structure, and a theorem that one can apply in such a context is the famed Cylinder Theorem:[28]

Theorem 0.1 *An elementary periodic orbit of a system with an integral I lies in a smooth cylinder of periodic solutions parameterized by I.*

Theorem 0.1 implies there exists a branch of periodic orbits in a system without a parameter, i.e. where $f : \mathbb{R}^n \to \mathbb{R}^n$. However the theory and algorithms developed in the previous section, and especially Equations 6 and 7, assume the system to be of the form $f : \mathbb{R}^n \times \mathbb{R} \to \mathbb{R}^n$, and cannot be applied in this case. To take advantage of the power of numerical continuation methods we must rephrase the problem in a form where such methods can be applied directly. We accomplish this with the addition of a "unfolding parameter". We only give an overview of these ideas here; for a full theoretical justification see Muñoz-Almaraz et al.[29] For further examples see Doedel,[6] Doedel et al.[7] and Zufiría.[36]

Consider the simple conservative system

$$\begin{aligned} x_1' &= x_2, \\ x_2' &= -x_1(1-x_1), \end{aligned} \tag{8}$$

which has the first integral $F = \frac{1}{2}x_2^2 + \frac{1}{2}x_1^2 - \frac{1}{3}x_2^3$. This set of equations is of the form $f : \mathbb{R}^n \to \mathbb{R}^n$ and has a branch of periodic orbits as shown in Figure 5.

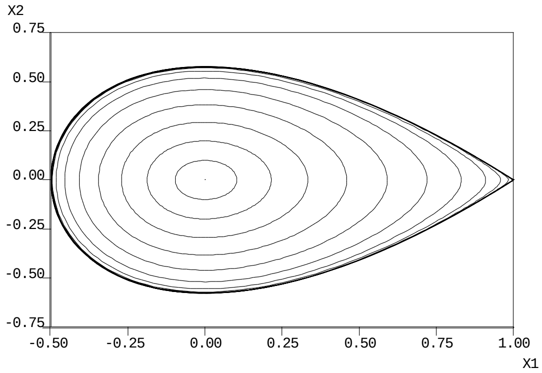

Figure 5: A family of periodic solutions of Equation 8.

We change Equation 8 into a problem of the form $f : \mathbb{R}^n \times \mathbb{R} \to \mathbb{R}^n$ by adding a new parameter and associated term:

$$\begin{aligned} x_1' &= x_2, \\ x_2' &= -x_1(1-x_1) + \lambda x_2. \end{aligned} \tag{9}$$

When $\lambda = 0$, Equations 8 and 9 are identical, and so have the same solutions. The idea is to add a term which destroys all the periodic solutions whenever the associated parameter is not zero. There are many such terms that one could add, e.g., we choose to add a term which is equivalent to damping.

Equation 9 is now of the desired form, and Figure 6 shows the bifurcation diagram we have computed for this system using λ as the bifurcation parameter. Each point on the bifurcation diagram represents a periodic solution, where the vertical axis is chosen to be a measure of the solution. In this case we have used the L2-norm of the solution, though there is a variety of quantities one could use instead, such as the maximum value of a component or the first integral I, to name a few. For $\lambda \neq 0$ there are no non-trivial periodic solutions, and at $\lambda = 0$ we find a *Hopf bifurcation* from which periodic orbits arise.

It is straightforward to detect Hopf bifurcations in a numerical continuation framework by examining the eigenvalue structure of the equations and looking for a complex conjugate pair of eigenvalues which pass through the imaginary axis as λ varies. In addition, in the neighborhood of a Hopf bifurcation one can derive analytic approximations to the family of periodic orbits. Using such an approximation as a starting guess, one can compute the entire branch of periodic solutions using the methods described in the previous section. Accordingly, we have computed the branch of periodic solutions emanating from $\lambda = 0$ and this branch is represented by the vertical branch in Figure 6.

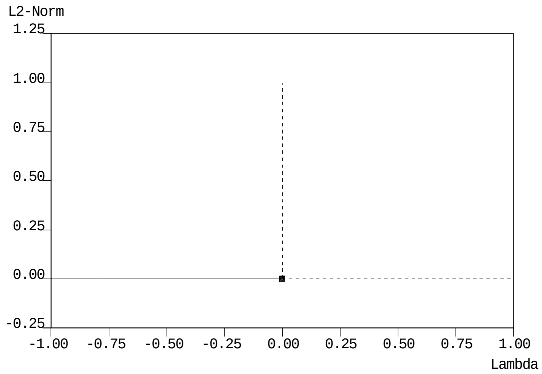

Figure 6: Bifurcation diagram for periodic solutions of Equation 9, computed using the pseudo-arclength continuation method. For $\lambda \neq 0$ there are no non-trivial periodic orbits. Each point on the vertical branch at $\lambda = 0$ corresponds to a periodic orbit such as those shown in Figure 5. The branch of non-trivial periodic orbits cannot be parameterized by the unfolding parameter λ, so natural continuation does not apply, but the pseudo-arclength method can be used readily to compute the solution branch.

The vertical branch of periodic solutions in Figure 6 may seem strange a first glance. On the other hand, it is clear that this branch must be vertical when plotted in these coordinates since, by construction, the periodic orbits we are computing only exist when $\lambda = 0$. The question now arises as to how such a branch may be computed using numerical continuation, since the vertical branch cannot be parameterized by λ. However we are not using natural parameter continuation in λ; rather we are using pseudo-arclength continuation. Equation 5 shows and Figure 3 illustrates that pseudo-arclength continuation is parameterized by the arclength along the curve, and not by the parameter λ. This is why the pseudo-arclength continuation method is able to follow the solution branch around the fold in Figure 3, where the branch is locally vertical. In the same way, the pseudo-arclength continuation method can even follow a globally vertical solution branch, whereas a natural continuation method could not.

THE CIRCULAR RESTRICTED 3-BODY PROBLEM IN THREE SPACE DIMENSIONS

The previous two sections described the mathematical formulation of problems that may be addressed by numerical continuation methods. In this section we show how the CR3BP can be expressed in the form of Equation 6. A derivation of the equations of motion can be found in Danby.[5]

The CR3BP describes the dynamics of a body with negligible mass under the gravitational influence of two massive bodies, called the primaries, where the primaries move in circular orbits about their barycenter. Let (x, y, z) denote the position of the negligible-mass body in a rotating barycentric coordinate system where the x-axis points from the larger to the smaller primary; the z-axis points along the orbit normal for the primaries; and the y-axis completes the right-handed orthogonal triad. The parameter μ represents the ratio of the mass of the smaller primary to the total mass. In this paper we consider the Earth-Moon system, for which $\mu = 0.01215$. The units are chosen so that the distance between the primaries, the sum of the masses of the primaries, and the angular velocity of the primaries are all equal to one. Consequently the larger and smaller primaries are located at $(-\mu, 0, 0)$ and $(1 - \mu, 0, 0)$ respectively. The equations of motion for the CR3BP are

$$\begin{aligned} \ddot{x} &= 2\dot{y} + x - (1-\mu)(x+\mu)r_1^{-3} - \mu(x-1+\mu)r_2^{-3}, \\ \ddot{y} &= -2\dot{x} + y - (1-\mu)yr_1^{-3} - \mu y r_2^{-3}, \\ \ddot{z} &= -(1-\mu)zr_1^{-3} - \mu z r_2^{-3}, \end{aligned} \tag{10}$$

where

$$r_1 = \sqrt{(x+\mu)^2 + y^2 + z^2}, \qquad r_2 = \sqrt{(x-1+\mu)^2 + y^2 + z^2}.$$

This dynamical system has one integral of motion, namely the energy

$$E = (v_x^2 + v_y^2 + v_z^2)/2 - U(x, y, z) - \mu(1-\mu)/2,$$

where

$$U = \frac{1}{2}(x_1^2 + x_2^2) + \frac{1-\mu}{d_1} + \frac{\mu}{d_2}.$$

It is well known that for each value of μ this system has five equilibria called Lagrange points (or libration points).[16,17,34] Three of the Lagrange points, denoted L1, L2 and L3, are collinear with the primary bodies; one of them, L1, lies between the two primaries. There exist two well-known families of periodic solutions near each of the collinear Lagrange points: the Lyapunov orbits that lie in the $x-y$ plane, and the so-called Vertical orbits that arise from the purely vertical solutions in the linearized dynamics.[22] In this paper we use numerical continuation methods to explore families of three-dimensional periodic solutions of Equation 10 that emanate from L1.

We make three modifications to Equation 10 to obtain a system to which AUTO2000 and numerical continuation may be applied. First, the three-dimensional second-order system in Equation 10 is rewritten as a six-dimensional first-order system in the standard way. This transformation is done as a convenience since AUTO2000 is set up to handle first-order systems. Second, we perform the transformation in Equation 7 where we add boundary conditions which impose unit periodicity, a phase condition constraint, and we introduce the unknown period T which we solve for as part of the numerical continuation procedure. Finally, we add a unfolding parameter as described in the previous section to turn the system into a mapping of the correct dimensions.

The resulting system of differential equations is

$$
\begin{aligned}
\dot{x} &= Tv_x + \lambda E_x, \\
\dot{y} &= Tv_y + \lambda E_y, \\
\dot{z} &= Tv_z + \lambda E_z, \\
\dot{v}_x &= T[2v_y + x - (1-\mu)(x+\mu)r_1^{-3} - \mu(x-1+\mu)r_2^{-3} + \lambda E_{v_x}], \\
\dot{v}_y &= T[-2v_x + y - (1-\mu)yr_1^{-3} - \mu y r_2^{-3} + \lambda E_{v_y}], \\
\dot{v}_z &= T[-(1-\mu)zr_1^{-3} - \mu z r_2^{-3} + \lambda E_{v_z}],
\end{aligned}
\tag{11}
$$

with separated boundary conditions

$$
\begin{aligned}
x(1) &= x(0), \quad & y(1) &= y(0), \quad & z(1) &= z(0), \\
v_x(1) &= v_x(0), \quad & v_y(1) &= v_y(0), \quad & v_z(1) &= v_z(0),
\end{aligned}
\tag{12}
$$

where T is the unknown period, and $\lambda \nabla E$ is the appropriate unfolding term as justified in Muñoz-Almaraz et al.[29]

TOUR OF THE BIFURCATION DIAGRAM

In this section we present a tour of the families of periodic orbits, emanating from L1, which we have computed using numerical continuation methods. Previous work has mapped portions of the families of periodic orbits for various values of μ; cf. Howell[22] and references therein. Some work has investigated bifurcations of these families, including Ichtiaroglou and Michalodimitrakis,[25] Hénon[20] and Howell and Campbell.[23] Our presentation is organized around the bifurcation diagram shown in Figure 7, in which each gray curve represents a branch of periodic solutions.

For reference, Figure 7 and later figures in this section show the Earth and Moon as two textured spheres. The five Lagrange points are visualized as cubes, and branches of periodic orbits emanate from each cube. For example, the branch of Lyapunov orbits, marked with an "L" and the branch of vertical orbits, marked with a "V", both emanate from the cube representing L1. Branch points, at which two branches intersect, are marked with small spheres. White spheres mark branch points at which both branches are shown and dark gray spheres mark branch points at which only one of the branches is shown. In addition, we include a gray rectangle that lies in the $x-y$ plane. Any solution branch that touches this rectangle has a planar solution at that point. For example, the entire branch of Lyapunov orbits is planar, so the entire line which represents the Lyapunov orbits touches the gray plane. We emphasize that, even though the various visualization aids are in the proper physical position with respect to each other, the solution branches themselves are only schematic. The relative positions of the various solution branches should not be interpreted as signifying any physical property of the solutions, other than those discussed above.

There are six families of periodic solutions illustrated in Figure 7. We first describe the connections between the branches. As mentioned before, the branch in Figure 7 labeled with an "L" emanating from L1 represents the Lyapunov orbits. On the branch of Lyapunov orbits there are two branch points, the first giving rise to the branch of Halo orbits labeled with an "H" (see Figures 12 and 13). On the curve of Vertical orbits, labeled with a "V", (see Figures 9 and 10) there is one branch point which gives rise to a branch of orbits, labeled with a "Y", which connects to the second branch point on the Lyapunov branch (see Figure 14). On the branch of Halo orbits there are two symmetry-related branch points giving rise to the "C" branch of orbits (see Figure 15). The "C" branch of orbits has two symmetry-related branch points which give rise to the "M" branch of orbits, which connects the Vertical orbits emanating from L4 and L5 (see Figures 16 and 17). There is a dark gray colored branch point on this branch through which one can reach L3 as well, though this branch is not discussed further here since our focus is L1.

Let us now examine the shapes of the periodic orbits associated with the various branches. We begin our tour of the periodic orbits by discussing several well-known branches which emanate from L1, as shown in Figure 8.[22] The plane labeled with "L" is comprised of Lyapunov orbits, with select individual orbits shown as curves. Similarly, the surface labeled with "V" is comprised of Vertical orbits and the surface labeled with "H" is comprised of Halo orbits.[4,13,15,18,21,24] The naming scheme is the same as used in Figure 7. As a visualization aid we show orbits which correspond to branch points, called *bifurcation orbits*, as thickened tubes. Accordingly, the thick curve which lies in the plane of the Lyapunov orbits is the orbit from which the Halos bifurcate. Note that, to reduce clutter in the diagram, we have only plotted the "northern" Halo orbits and not the "southern" Halo orbits. related through the symmetry $z \to -z$.

We now turn our attention to the Vertical orbits. In Figure 9 we show the Vertical orbits from their origin at L1 up to the first branch point. In this and all following figures in this section the bifurcation diagram from Figure 7 is shown on the right, with the appropriate section labeled with a white arrow. As before, the bifurcation orbit is show as a thickened tube. Similarly, Figures 10 and 11 show the branch of Vertical orbits starting at the first branch point. As can be seen, these orbits grow to encompass the Earth, and end in a period-doubling bifurcation to a branch of planar solutions. Accordingly, the branch in Figure 7 touches the gray plane in two places; the first corresponding to the creation of the branch at L1 and the second at the period-doubling bifurcation to the planar solutions marked with a dark gray sphere. These doubly symmetric solutions are described in Bray and Goudas[3] and Zagouras and Kazantzis.[35] Because these orbits provide a view of the poles of one or both primaries, they might be useful for polar science missions.[14]

There is one branch point on the branch of Vertical solutions, and using parameter continuation methods it is a simple matter to compute the bifurcating branch. As can be seen in Figure 14 the "Y" branch of orbits connects the Lyapunov and Vertical branch. The orbits themselves are shown in the same figure. The plane is a collection of Lyapunov orbits and the thick curve in the plane is the second branch point on the Lyapunov branch. The other thick curve is the first branch point on the Vertical branch, as shown in Figure 9. There is a second symmetry-related branch not shown here, and the whole branch of orbits forms a loop as shown in Figure 7. Some of the orbits on the "Y" branch were plotted in Zagouras and Kazantzis[35] for $\mu = 0.00095$.

The first branch point on the Lyapunov branch gives rise to the well known Halo orbits. Figure 12 shows a selection of northern Halo orbits between the branch point on the Lyapunov branch from which they arise up to the first branch point on the Halo branch itself. We have removed the surface of orbits from this figure in order to make the two bifurcation orbits easier to distinguish. Figure 13 begins where Figure 12 ends and shows the northern Halo orbits from the first branch point on the Halo branch up to the second branch point which gives rise to a planar branch of solutions marked with a dark gray sphere, not shown here. As can be seen in Figure 7 the Halo branch can be continued past the branch point to the planar solutions and gives rise to the symmetry-related branch of southern Halos. Accordingly, the branch of Halo orbits in Figure 7 is a loop.

At this point the connectivity of the bifurcation diagram becomes quite complex. On the branch of Halo orbits there are two symmetry-related branch points. The branch points are connected by the loop of orbits shown in Figure 7 and labeled with a "C". Two additional symmetry-related branch points occur on the "C" branch, and they give rise to the "M" branch which twice intersects the "C" loop transcritically.

On the "C" branch there are four symmetry-related segments separated by the four branch points. Figure 15 shows a representative collection of orbits on the "C" branch from one of these segments. The other segments have the same structure as Figure 15 except that they are reflected across the the $x - y$ plane and/or the $x - z$ plane. The branch point from Figure 12 is indicated with the white arrow and a small thick orbit. The thick figure-eight orbit in the middle of the figure is a bifurcation orbit and connects with the "M" branch.

The "M" branch of orbits is of particular interest in that it connects the "vertical" orbits from L4 with the "vertical" orbits from L5.[26] In fact, the "vertical" orbits of L4 and L5 are on the same branch of orbits. The "M" branch of orbits transcritically intersects the "C" branch of orbits in two places, and there is a third branch point in between these two (shown as the dark gray sphere in Figure 7).

Figure 16 shows a representative collection of orbits emanating from L4 which are very similar to the Vertical orbits which emanate from L1. The thick curve is the same bifurcation orbit as shown in Figure 15, and is the first branch point one encounters on the "C" branch as one moves away from L4.

Figure 17 shows a representative collection of orbits between the figure-eight branch point show in Figures 15 and 16. The thick orbit, which encompasses the Earth, is a branch point which connects to the "vertical" orbits of L3, though this calculation is not shown here. This is the branch point that is shown in dark gray. If you continue on the "M" branch past the dark gray branch point you arrive at a symmetry-related branch of "vertical" orbits for L5. This branch is comprised of the symmetric version of Figures 16 and 17 reflected through the $x - z$ plane.

For the N-body problem, the Mirror Theorem[32] states that an orbit is periodic if a mirror configuration occurs at two distinct epochs. This is not a necessary condition for periodicity, but the Mirror Theorem has been a effective tool for computing periodic solutions near collinear Lagrange points. Robin and Markellos[31] noted that in the CR3BP there are only two types of mirror configurations. In the (P) (or planar) configuration, the orbit crosses the $x - z$ plane orthogonally; in the (A) (or axial) configuration, the orbit crosses the x axis orthogonally. In Howell[21] and Howell and Campbell,[23] periodic orbits were determined by a two-point boundary value problem where each boundary condition describes a (P) configuration. In the present study we do not exploit the Mirror Theorem in the definition of the boundary conditions. Nonetheless it is interesting to examine the periodic orbits we found in light of the Mirror Theorem. A (P) configuration, together with the symmetry $y \to -y$, $t \to -t$ of the dynamics in Equation 10, implies that the orbit is symmetric across the $x - z$ plane. An (A) configuration, together with the symmetry $y \to -y$, $z \to -z$, $t \to -t$ of the dynamics, implies that the orbit is symmetric with respect to rotation about the x axis through an angle of 180 degrees. Let us call the symmetry $y \to -y$, $t \to -t$ the *reflective* symmetry, and call the symmetry $y \to -y$, $z \to -z$, $t \to -t$ the *rotational* symmetry. An orbit with both reflective symmetry and rotational symmetry and called *doubly symmetric.* The composition of the reflective and rotational symmetries implies that a doubly symmetric orbit is also symmetric with respect to reflection across the $x - y$ plane. In Figure 8 we see that each Lyapunov orbit is doubly symmetric in a trivial way. Each Vertical orbit in Figures 8-11 shows that the Vertical orbits have a more interesting doubly symmetric structure. Each Halo orbits in Figures 8, 12 and 13 exhibits the reflective symmetry, but not the rotational symmetry. By contrast, the "Y" orbits in Figure 14 lack the reflective symmetry. However each"Y" orbit in Figure 14 does have two (A) configurations, and so is rotationally symmetric. The "C" and "M" orbits in Figures 15-17 have neither (P) nor (A) configurations in general, with the exception of the Vertical-like L45 orbit in Figure 17. As a consequence, the "C" and "M" branches could not be found using the Mirror Theorem.

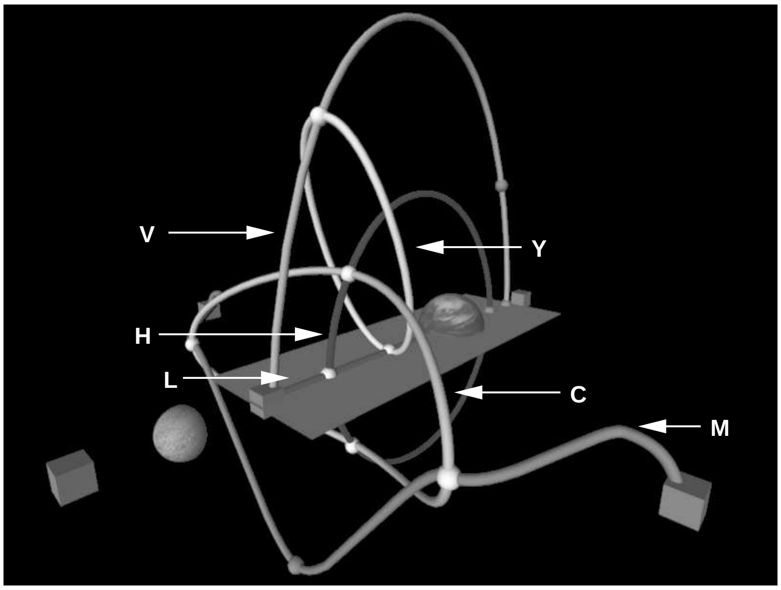

Figure 7: The bifurcation diagram for periodic orbits emanating from L1: The gray curves represent the various branches of periodic solutions computed using numerical continuation methods. The Earth and Moon are shown as two textured spheres, and the five Lagrange points are shown as cubes. The branch labeled "L" represents the Lyapunov orbits and the branch labelled "V" represents the Vertical orbits (see Figures 9 , 10, and 11). The rectangle lie in the $x - y$ plane, and has the property that any solution branch which touches it has a planar solution at that point. For example, the entire branch of Lyapunov orbits lie in the plane, so all the orbits on that branch are planar. On the branch of Lyapunov orbits there are two branch points, the first giving rise to the branch of Halo orbits, labelled with "H" (see Figures 12 and 13), and the second giving rise to a branch of orbits which connects the Lyapunov and Vertical branches, labelled with "Y" (see Figure 14). On the branch of Halo orbits there are two symmetry-related branch points giving rise to the branch of orbits labelled with "C" (see Figure 15). The "C" branch of orbits has two symmetry-related simple branch points which give rise to the branch of orbits labelled with "M", which connects the "vertical" orbits emanating from L4 and L5 (see Figures 16 and 17). There is a dark gray branch point on this branch through which one can reach L3 as well, though this branch is not discussed further here. Throughout this section the above naming scheme is used for all orbits.

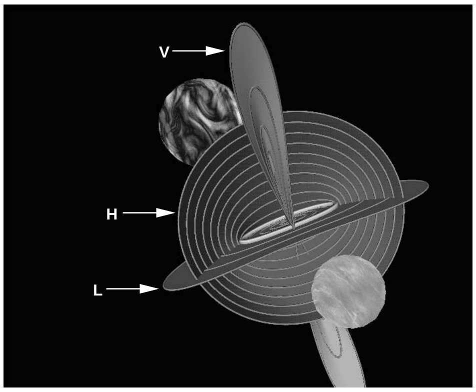

Figure 8: Some well-known periodic orbits near L1: The plane labelled with the "L" is comprised of Lyapunov orbits, with select individual orbits shown as curves. Similarly, the surface labelled with "V" is comprised of Vertical orbits and the surface labelled with a "H" is comprised of Halo orbits. The naming scheme is the same as used in Figure 7. The thick curve in the plane of the Lyapunov orbits is the orbit from which the Halos bifurcate. There is another symmetry-related branch of southern Halo orbits which is not shown in this diagram.

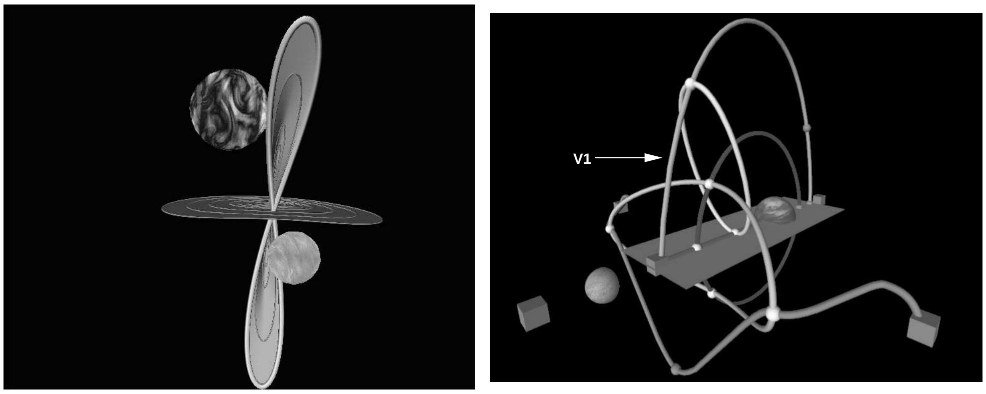

Figure 9: The Vertical orbits up to the first branch point: The surface on the left contains all of the vertical orbits up to the first bifurcation orbit, which is shown as a thick curve. The part of the bifurcation diagram where these orbits are found is labelled as "V1".

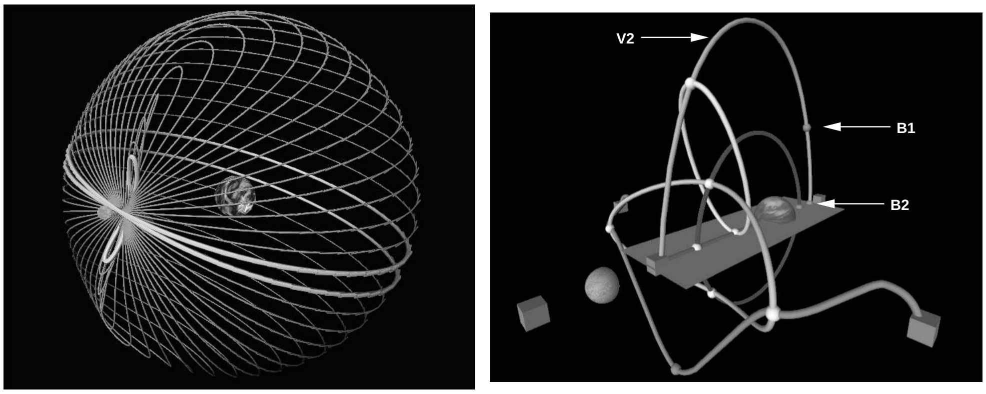

Figure 10: An overall view of the Vertical orbits after the first branch point: The curves are a representative collection of Vertical orbits. As in Figure 9 the bifurcation orbit is shown as a thick curve and can be found on the left side of the picture near the Moon. The other thick curve that encompasses the Earth and lies close to the $x - y$ plane is a solution close to a period-doubling bifurcation, marked "B2" in the bifurcation diagram, from which emanates, via reverse period-doubling, a branch of planar solutions that we do not follow here. There is a second branch point in this figure, marked "B1", which we do not follow either. The part of the bifurcation diagram where these orbits are found is labelled as "V2".

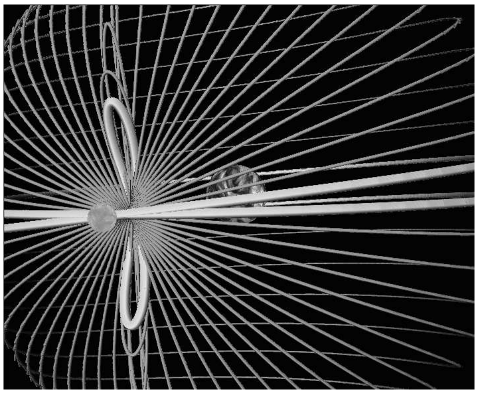

Figure 11: A closeup view of the Vertical orbits past the first branch point: The curves are a representative collection of orbits. As in Figure 9, the bifurcation orbit is shown as a thick curve and can be found to the left of the picture near the Moon. This is a closeup version of Figure 10.

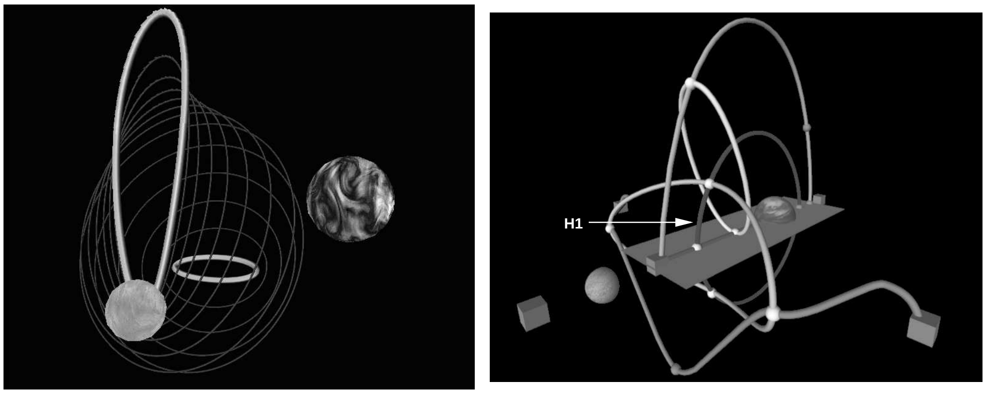

Figure 12: The Halo orbits up to the first branch point: The curves are a representative collection of orbits from the northern branch of Halo orbits. The thick orbit between the Earth and Moon is the Lyapunov orbit from which the Halo orbits bifurcate. The thick orbit near the Moon is the first bifurcation orbit on the branch of Halo orbits. The part of the bifurcation diagram where these orbits are found is labelled "H1".

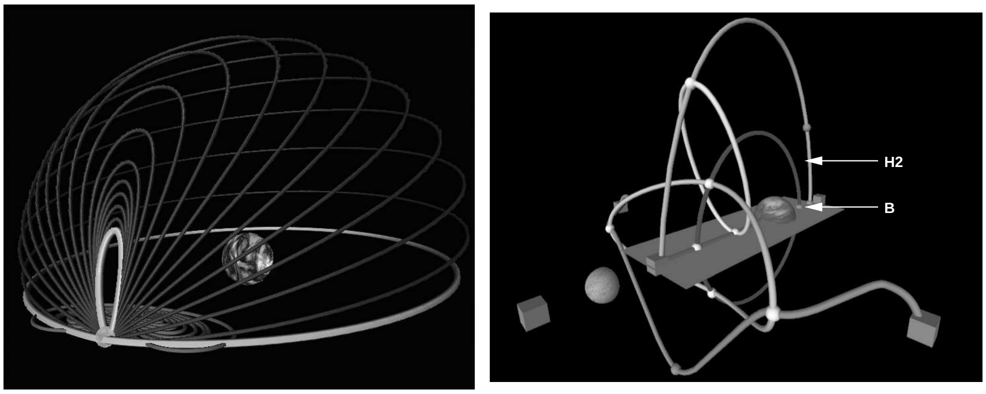

Figure 13: The Halo orbits after the first branch point: The curves are a representative collection of orbits from the first branch point on the branch of northern Halo orbits up to the second branch point. A set of Lyapunov orbits is shown for reference. The part of the bifurcation diagram where these orbits are found is labelled as "H2". The thick orbit near the Moon is the first bifurcation orbit on the branch of Halo orbits. The blue curve which encompasses the Earth is a bifurcation orbit, marked "B" in the bifurcation diagram, to a branch of planar orbits which is not shown here. Once you pass through the above branch point, you enter the symmetry-related branch of southern Halo orbits. Hence, the blue branch of Halo orbits in Figure 7 is a loop.

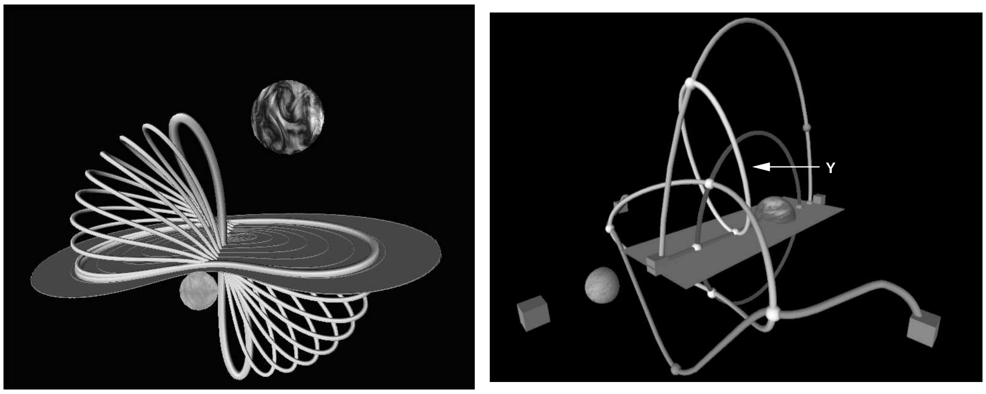

Figure 14: A branch of orbits connecting the Lyapunov and Vertical orbits: The planar shape is a collection of Lyapunov orbits and the thick curve on the plane is the second bifurcation orbit on the Lyapunov branch. The thick Vertical orbit is the first bifurcation orbit on the Vertical branch, as shown in Figure 9. The curves are a representative collection of orbits which connect these two branch points. There is a second symmetry-related branch not shown here which consists of these above orbits reflected across the $x-z$ plane. Accordingly, the whole branch of orbits forms a loop as shown in Figure 7. The part of the bifurcation diagram where these orbits are found is labelled as "Y".

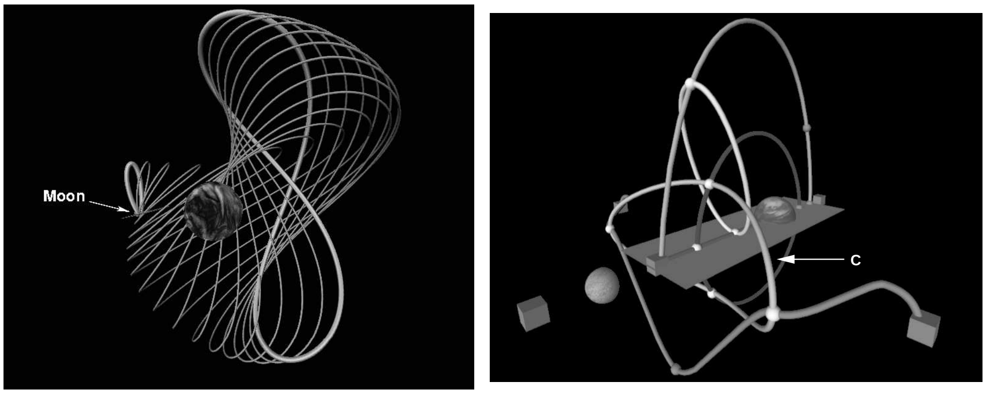

Figure 15: A branch of orbits emanating from the first branch point on the Halo branch: The curves are a representative collection of orbits. The branch point from Figure 12 is indicated with the white arrow and a small thick orbit. The thick figure-eight orbit in the middle of the figure is a bifurcation orbit and connects with a branch of "vertical" like orbits which emanates from L4. The part of the bifurcation diagram where these orbits are found is labelled as "C".

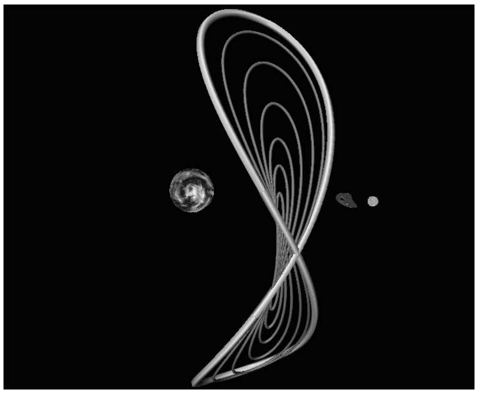

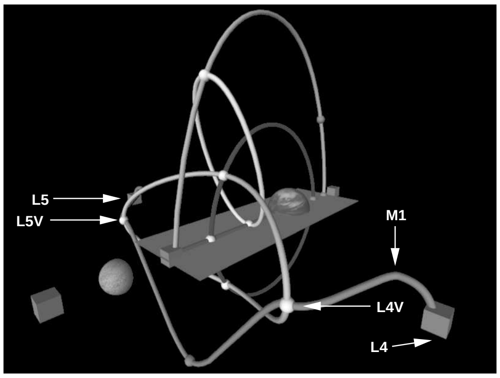

Figure 16: The L4 "vertical" orbits: The curves are a representative collection of orbits emanating from L4 which are very similar to the Vertical orbits which emanate from L1. The thick curve is the same bifurcation orbit shown in Figure 15. There are two branches of such orbits and the one shown here can be found on the bifurcation diagram between the white arrows labelled "L4" and "L4V". The other branch is found on the bifurcation diagram between the white arrows labelled "L5" and "L5V". The part of the bifurcation diagram where these orbits are found is labelled as "M1".

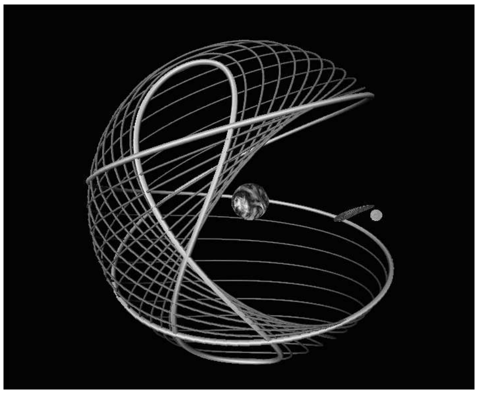

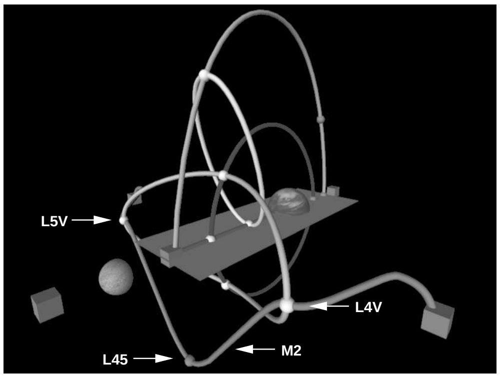

Figure 17: Connection between L3, L4 and L5 "vertical" orbits: The curves are a representative collection of orbits between the figure-eight bifurcation orbit shown in Figures 15 and 16. The section of the bifurcation diagram where these orbits occur is between the arrows labelled "L4V" and "L45". The thick orbit, which encompasses the Earth, is the bifurcation orbit labelled "L45". This bifurcation connects to the "vertical" orbits of L3, though this branch is not shown here. If one continues on this branch past the above branch point one computes a symmetry-related branch of "vertical" orbits for L5, between the arrows labelled "L5V" and "L45" including the symmetric version of Figure 16 emanating from L5. The part of the bifurcation diagram where these orbits are found is labelled as "M2".

CONCLUSION

In this paper we have shown how numerical continuation methods may be applied to the computation of periodic orbits in the CR3BP. Pseudo-arclength continuation provides a robust method for computing periodic orbits which neither depends on the Mirror Theorem[32] nor upon any expansions about the equilibria from which the solution arise. Accordingly, we are able to compute periodic orbits of arbitrary extent and follow all simple bifurcation points in the bifurcation diagram for L1.

Numerical continuation is a subject with a broad literature and we have provided here only the barest introduction. For further details we encourage the reader to see citations in the bibliography. We note that the general theory of numerical continuation is not trivially applicable to conservative systems, such as the CR3BP, but that one may reformulate the problem with the addition of a unfolding parameter.

Once the CR3BP has been reformulate, it is straightforward to compute the families of periodic orbits emanating from the L1 Hopf bifurcation. The connectivity of this bifurcation diagram is intricate, and actually includes connections to other Lagrange points. Since our focus for this paper has been L1 we have only shown a small part of a much larger bifurcation diagram.

Some of the orbits computed in this study might be useful for scientific missions. However, the CR3BP neglects some important effects in the full force model, including the eccentricity of the primaries, third-body gravitational forces and solar radiation pressure. In future work it would be interesting to determine how much a trajectory in a full force model, propagated from an initial state found in this study, differs from the corresponding CR3BP periodic orbit. In particular we would like to know the delta-V budget required to remain near the nominal CR3BP orbit. As a further extension of this work, we would like to exploit numerical continuation methods, and invariant manifolds associated with these orbits, to determine efficient ways to insert a spacecraft into such an orbit.

ACKNOWLEDGMENTS

EJD and RCP would like to thank Herb Keller for initially getting us interested in this problem and for his support of this work. In addition, this work has been supported by the National Science Foundation through the grant KDI/NCC Molecular information and computer modeling in electrophysiology, SBR-9873173. EJD is also supported by NSERC (Canada) Research Grant A4274. DJD thanks Eric Campbell, John Carrico, Dave Folta, Kathleen Howell and Karen Richon for enlightening discussions.

References

[1] E. L. Allgower and K. Georg. Numerical path following. In P. G. Ciarlet and J. L. Lions, editors, *Handbook of Numerical Analysis*, volume 5. North Holland Publishing, 1996.

[2] U. M. Ascher, J. Christiansen, and R. D. Russell. Collocation software for boundary value ODEs. *ACM Trans. Math. Software*, 7:209–222, 1981.

[3] T. A. Bray and C. L. Goudas. Doubly symmetric orbits about the collinear Lagrangian points. *The Astronomical Journal*, 72(2):202–213, 1967.

[4] J. V. Breakwell and J. V. Brown. The 'Halo' family of 3-dimensional periodic orbits in the Earth-Moon restricted 3-body problem. *Celestial Mechanics*, 20:389–404, 1979.

[5] J. M. A. Danby. *Fundamentals of Celestial Mechanics*. Willmann-Bell, 1992.

[6] E. J. Doedel. AUTO, a program for the automatic bifurcation analysis of autonomous systems. *Congr. Numer.*, 30:265–384, 1981.

[7] E. J. Doedel, D. G. Aronson, and H. G. Othmer. The dynamics of coupled current-biased Josephson junctions II. *Int. J. Bifurcation and Chaos*, 1(1):51–66, 1991.

[8] E. J. Doedel, A. R. Champneys, T. F. Fairgrieve, Y. A. Kuznetsov, B. Sandstede, and X.-J. Wang. AUTO97: Continuation and bifurcation software for ordinary differential equations. Technical report, Department of Computer Science, Concordia University, Montreal, Canada, 1997. (Available by FTP from ftp.cs.concordia.ca in directory pub/doedel/auto).

[9] E. J. Doedel, H. B. Keller, and J. P. Kernévez. Numerical analysis and control of bifurcation problems: (I) Bifurcation in finite dimensions. *Int. J. Bifurcation and Chaos*, 1:493–520, 1991.

[10] E. J. Doedel, H. B. Keller, and J. P. Kernévez. Numerical analysis and control of bifurcation problems: (II) Bifurcation in infinite dimensions. *Int. J. Bifurcation and Chaos*, 1:745–772, 1991.

[11] E. J. Doedel and R. C. Paffenroth. The AUTO2000 command line user interface. In *Proceedings of the 9th International Python Conference*, pages 233–241, March 2001.

[12] E. J. Doedel, R. C. Paffenroth, J. Galán, H. B. Keller, and A. Vanderbauwhede. Continuation of periodic solutions in conservative systems with application to the 3-body problem. preprint.

[13] R. W. Farquhar and A. K. Kamel. Quasi-periodic orbits about the translunar libration point. *Celestial Mechanics*, 7:458–473, 1973.

[14] D. Folta, Young C., and Ross A. Unique non-Keplerian orbit vantage locations for Sun-Earth connections and Earth Science Vision roadmaps. In *NASA Goddard Flight Dynamics Symposium*, 2001.

[15] G. Gómez, Á. Jorba, J. Marsdemont, and C. Simó. Study of the transfer from the earth to a halo orbit around the equilibrium point l_1. *Celestial Mechanics and Dynamical Astronomy*, 56:541–562, 1993.

[16] G. Gómez, J. Llibre, R. Martínez, and C. Simó. *Dynamics and Mission Design Near Libration Points, Vol. II: Fundamentals: The Case of Triangular Libration Points*, volume 3. World Scientific, 2001.

[17] G. Gómez, J. Llibre, R. Martínez, and C. Simó. *Dynamics and Mission Design Near Libration Points, Volume I: Fundamentals : The Case of Collinear Libration Points*, volume 2. World Scientific, 2001.

[18] G. Gómez, J. Masdemont, and C. Simó. Lissajous orbits around halo orbits. In *AAS/AIAA Space Flight Mechanics Meeting*, 1997. AAS 97-106.

[19] M. Henderson. Multiple parameter continuation: Computing implicitly defined k-manifolds. *Int. J. Bifurcation and Chaos*, 2001. (to appear).

[20] M. Hénon. *Generating Families in the Restricted Problem*. Springer-Verlag, 1997.

[21] K. C. Howell. Three-dimensional, periodic, 'Halo' orbits. *Celestial Mechanics*, pages 53–71, 1984.

[22] K. C. Howell. Families of orbits in the vicinity of the collinear libration points. In *AIAA/AAS Astrodynamics Specialist Conference*, 1998. AAS 98-4465.

[23] K. C. Howell and E. T. Campbell. Three-dimensional periodic solutions that bifurcate from Halo families in the circular restricted three-body problem. In *Spaceflight Mechanics*, 1999. AAS 99-161.

[24] K.C. Howell and R.W. Farquhar. John Breakwell, the restricted problem, and Halo orbits. *Acta Astronautica*, 29:485–488, 1993.

[25] S. Ichtiaroglou and M. Michalodimitrakis. Three-body problem: The existence of families of three-dimensional periodic orbits. *Astronomy and Astrophysics*, 81:30–32, 1980.

[26] Á Jorba and J. Villanueva. Stability and asymptotic behavior of the vertical family of periodic orbits around l_5 of the restricted three body problem. In *Actas del XV CEDYA / V CMA*, pages 303–308. Universidad de Vigo, 1998.

[27] H. B. Keller. Numerical solution of bifurcation and nonlinear eigenvalue problems. In P. H. Rabinowitz, editor, *Applications of Bifurcation Theory*, pages 359–384. Academic Press, 1977.

[28] K. R. Meyer. *Periodic Solutions of the N-Body Problem.* Springer, 1999.

[29] F. J. Muñoz Almaraz, E. Freire, E. J. Doedel, A. Vanderbauwhede, and J. Galán. Continuation of periodic orbits in conservative and Hamiltonian systems. preprint.

[30] W. C. Rheinboldt. *Numerical analysis of parametrized nonlinear equations.* Wiley-Interscience, 1986. University of Arkansas Lecture Notes in the Mathematical Sciences.

[31] I.A. Robin and V.V. Markellos. Numerical determination of the three-dimensional periodic orbits generated from vertical self-resonant satellite orbits. *Celestial Mechanics*, 21:395–434, 1980.

[32] A. E. Roy. *Orbital Motion.* Adam Hilger, 1988.

[33] R. D. Russell and J. Christiansen. Adaptive mesh selection strategies for solving boundary value problems. *SIAM J. Numer. Anal.*, 15:59–80, 1978.

[34] V. Szebehely. *Theory of Orbits: The Restricted Problem of Three Bodies.* Academic Press, 1967.

[35] C.G Zagouras and P.G. Kazantzis. Three-dimensional periodic oscillations generating form plane periodic ones around the collinear Lagrangian points. *Astrophysics and Space Science*, 61:389–409, 1979.

[36] J. A. Zufiría. PhD thesis, Applied Mathematics, California Institute of Technology, 1987.